Synaptic effects of mutations in neuronal Cav2.1 calcium channels

Kaja, S.

6

Severely Impaired Neuromuscular Synaptic Transmission Causes Muscle Weakness in the *Cacna1a* Mutant Mouse *Rolling Nagoya*

Simon Kaja,[1,2] Rob C.G. Van de Ven,[3] J. Gert van Dijk,[1]
Jan J.G.M. Verschuuren[1], Kiichi Arahata,[4†] Rune R. Frants,[3]
Michel D. Ferrari,[1] Arn M.J.M. van den Maagdenberg,[1,3]
and Jaap J. Plomp[1,2]

Department of [1]Neurology and Clinical Neurophysiology, [2]Molecular Cell Biology - Group Neurophysiology and [3]Human Genetics, Leiden University Medical Centre, Leiden, The Netherlands;
[4]Department of Neuromuscular Research, National Institute of Neuroscience, NCNP, Kodaira, Japan.
[†]deceased

Submitted

Abstract

The ataxic mouse *rolling Nagoya* (RN) carries a missense mutation in the *Cacna1a* gene, encoding the pore-forming subunit of neuronal $Ca_V2.1$ (P/Q-type) Ca^{2+} channels. Besides being the predominant type of Ca_V channel in the cerebellum, $Ca_V2.1$ channels mediate acetylcholine (ACh) release at the peripheral neuromuscular junction (NMJ). Therefore, $Ca_V2.1$ dysfunction induced by the RN mutation may disturb ACh release at the NMJ. The dysfunction may resemble the situation in Lambert-Eaton myasthenic syndrome (LEMS), in which auto-antibodies target $Ca_V2.1$ channels at NMJs, inducing severely reduced ACh release resulting in muscle weakness. We tested neuromuscular function of RN mice and characterized transmitter release properties at their NMJs in diaphragm, soleus and flexor digitorum brevis muscles. Clinical muscle weakness and fatigue was demonstrated using repetitive nerve-stimulation electromyography, grip strength testing and an inverted grid hanging test. Muscle contraction experiments showed a compromised safety factor of neuromuscular transmission. In *ex vivo* electrophysiological experiments we found severely impaired ACh release. Compared to wild-type, RN NMJs have 50-75% lower nerve stimulation-evoked transmitter release, explaining the observed muscle weakness. Surprisingly, the reduction in evoked release was accompanied by a ~3-fold increase of spontaneous ACh release. This synaptic phenotype suggests a complex effect of the RN mutation on different functional $Ca_V2.1$ channel parameters, presumably with a positive shift of activation potential as the prevailing feature. Taken together, our studies indicate that the gait abnormality of RN mice is due to a combination of ataxia and muscle weakness and that RN models aspects of the NMJ dysfunction in LEMS.

A preliminary part of this study has been presented at the Xth International Conference on Myasthenia Gravis and Related Disorders (2002, Key Biscayne, FL, USA), and has been included in a 'poster-paper' (Plomp et al., 2003).

Acknowledgements
We thank Ulrike Nehrdich for excellent caretaking of the *rolling Nagoya* breeding and Paul Adams for insightful discussions on $Ca_V2.1$ channels. This work was supported by grants from the Prinses Beatrix Fonds (#MAR01-0105), the Hersenstichting Nederland (#9F01(2).24, to J.J.P.), the KNAW van Leersumfonds (to J.J.P.), the Organisation for Scientific Research (NWO; Vici 918.56.602, to M.D.F), the European Union ("Eurohead" grant LSHM-CT-2004-504837, to M.D.F, R.R.F and A.M.J.M.v.d.M), and the Center for Medical Systems Biology (CMSB), established by the Netherlands Genomics Initiative/NWO.

Introduction

The natural mutant mouse *rolling Nagoya* (RN) (Oda, 1973) displays a severely ataxic gait. It carries a recessive point mutation in the *Cacna1a* gene on chromosome 8, causing an R1262G amino acid change in the voltage-sensing S4 segment of the third transmembrane repeat of the encoded pore-forming subunit of $Ca_V2.1$ (P/Q-type) voltage-gated Ca^{2+} channels (Mori et al*.,* 2000). These neuronal channels are expressed widely throughout the central nervous system (CNS) and play a crucial role in neurotransmitter secretion from nerve terminals (Wheeler et al., 1995; Catterall et al., 2003). In the mammalian peripheral nervous system, expression of $Ca_V2.1$ channels is largely restricted to the neuromuscular junction (NMJ), where they mediate acetylcholine (ACh) release from the motor nerve terminal (Uchitel et al., 1992; Bowersox et al., 1995; Hong and Chang, 1995; Lin and Lin-Shiau, 1997).

Mutations in the human *CACNA1A* gene on chromosome 19 have been identified in several human neurological disorders, such as familial hemiplegic migraine type 1 (FHM1), episodic ataxia type 2 (EA2), spinocerebellar ataxia type 6 (SCA6), as well as forms of epilepsy (Ophoff et al., 1996; Zhuchenko et al., 1997; Jouvenceau et al., 2001; Imbrici et al., 2004). Recently, we have generated and analysed a *Cacna1a* knockin mouse, carrying the FHM1 mutation R192Q (Van Den Maagdenberg et al., 2004; Kaja et al., 2005). *Tottering* and *leaner* are natural *Cacna1a* mutant mouse strains*,* which share an ataxic phenotype with RN but in addition display epilepsy (Fletcher et al., 1996; Doyle et al., 1997). Furthermore, *Cacna1a* null-mutant mice have been generated, which are severely ataxic and epileptic and die young (Jun et al., 1999; Fletcher et al., 2001).

Besides affecting CNS synapse function (for reviews see Plomp et al., 2001; Felix, 2002; Pietrobon, 2005b), human and mouse *CACNA1A* mutations most likely influence ACh release at the NMJ. For instance, reduced ACh release may cause muscle weakness, similar to the Lambert-Eaton myasthenic syndrome (LEMS) in which auto-immune antibodies target $Ca_V2.1$ channels (Lennon et al*.,* 1995). In muscle biopsies of EA2 patients, NMJ dysfunction has been shown with *in vivo* electromyography and *ex vivo* micro-electrode analysis (Jen et al*.,* 2001; Maselli et al*.,* 2003a). In contrast, no electromyographical deficits were found in SCA6 patients (Jen et al*.,* 2001; Schelhaas et al*.,* 2004) and in FHM1 patients with the *CACNA1A* mutation I1811L (Terwindt et al*.,* 2004).

We previously investigated NMJ dysfunction in *tottering* and R192Q knockin mice and found increased spontaneous ACh release, normal evoked release at low rate stimulation, and a more pronounced rundown of evoked release at high rate stimulation (Plomp et al., 2000; Van Den Maagdenberg et al., 2004; Kaja et al., 2005). However, no ensuing muscle weakness was present, due to the large safety factor of transmission at the NMJ (Wood and Slater, 2001). Here, we investigated NMJ function of RN mice with *in vivo* and *ex vivo* electrophysiological methods and observed profound functional synaptic changes leading to muscle weakness, with similarity to LEMS.

Materials and methods

Mice

Male and female mice were used at ~3 months of age. RN mice had ~25% lower body weight than wild-type littermates, while heterozygous animals were normal (25.6 ± 0.7, 26.4 ± 1.1 and 19.3 ± 0.9 g for wild-type, heterozygous and homozygous RN mice, respectively, n=7-10, $p<0.001$).

For *ex vivo* experiments, mice were euthanized by carbon dioxide inhalation. Phrenic nerve-hemidiaphragms, soleus and flexor digitorum brevis (FDB) muscles were dissected and mounted in standard Ringer's medium (in mM: NaCl 116, KCl 4.5, $CaCl_2$ 2, $MgSO_4$ 1, NaH_2PO_4 1, $NaHCO_3$ 23, glucose 11, pH 7.4) at room temperature and continuously bubbled with 95% O_2 / 5% CO_2.

All *ex vivo* experiments were carried out with the investigator blinded to the genotype. The experiments had been approved by the Leiden Experimental Animal Committee and were conducted in accordance with Dutch law and Leiden University guidelines.

Genotyping

Genotyping for the RN mutation was performed by PCR using primers P207 (5'- GGTG-CACACCACTATGTTTC -3') and P221 (5'- ACGACCTCTAAAGACCACCAAG -3') on genomic DNA from tail tissue, similar to protocols described before (Plomp et al*.,* 2000). After PCR, the 145 base-pair products were digested with restriction enzyme *Sty*I according to recommendations of the supplier and electrophoresed on a 3% agarose gel. RN product yielded fragments of 137 and 18 bps, whereas the wild-type product remained uncut.

Grip strength assessment

Muscle strength was measured using a grip strength meter for mice (600 g range; Technical and Scientific Equipment GmbH, Bad Homburg, Germany), connected to a laptop computer. The test was carried out essentially as originally described for rats (Tilson and Cabe, 1978). Mice were held on the base of the tail and allowed to firmly grab the pulling bar of the device with both forepaws. The mouse was then pulled gently backwards until it released its grip. The peak force of each trial was considered the grip strength. Each mouse performed five trials, approx. 30 s apart. The averaged value of the trials was used for statistical analysis.

Inverted grid hanging test

Fatigability of limbs was tested for with the inverted grid hanging test (Karachunski et al*.,* 1995). A mouse was placed on the centre of an invertible 40x40 cm wire grid, mounted ~80 cm above a padded surface. After gently inverting the grid, the time was recorded that the mouse was able to hang on, with a maximum of 5 min. Each mouse was tested three times with ~30 min interval. The average hanging times were calculated for each mouse.

Repetitive nerve stimulation electromyography (RNS-EMG)

Mice were anaesthetised with a 15:1 (v/v) mixture of ketamine hydrochloride (Ketalar®; 10 mg/ml, Parke-Davis, Hoofddorp, The Netherlands) and medetomidine hydrochloride (Domitor®; 1 mg/ml, Pfizer, Capelle a/d IJssel, The Netherlands), at 8 µl per g body weight administered intraperitoneally.

Subcutaneous recording needles were inserted in the plantar aspect of the hind foot, and stimulation needle electrodes were inserted near the sciatic nerve in the thigh. Using a portable Nicolet Viking Quest EMG apparatus (Nicolet Biomedical, Madison, WI), the compound muscle action potential (CMAP) from foot muscles was recorded following supramaximal nerve stimulation (150% of the stimulus intensity giving a just maximal response). Trains of 10 stimuli were applied at increasing frequencies of 0.2, 1, 3, 5 and 10 Hz, with a 2-minute recovery period between each train. Thereafter the 0.2 Hz stimulation protocol was repeated in order to confirm that shape and amplitude of the CMAP were similar to that in the beginning of the protocol, thereby excluding any changes due to possible fatigue or electrode displacement. We could not reliably test stimulation frequencies higher than 10 Hz because of movement artefacts.

Data was analysed in a custom-written Matlab (The MathWorks Ics., Natick, MA) analysis routine, performing base-line correction as well as spline interpolation. CMAP amplitude and area of the initial negative peak were measured for all CMAPs in a train. The largest decrease ('maximal decrement') of amplitude and area during the train was identified and expressed as a percentage of the value of the first CMAP in that train.

Ex vivo *muscle contraction experiments*

Left phrenic nerve-hemidiaphragm preparations were mounted in a dish containing 10 ml Ringer's medium at room temperature (20-22 °C), continuously bubbled with 95% O_2 / 5% CO_2. The central tendon was connected via a metal hook and a string to a K30 force transducer (Harvard Apparatus, March-Hugstetten, Germany). The signal was amplified by a TAM-A bridge-amplifier (Harvard Apparatus) and digitized by a Digidata 1200B digitizer (Axon Instruments, Union City, USA), connected to a personal computer running Axoscope 9.0 data-acquisition software (Axon Instruments). The nerve was placed on a bipolar stimulation electrode. Supramaximal stimuli (usually ~10 V) of 100 μs duration were delivered every 10 min for 3 s at 40 Hz from a Master-8 programmable stimulator (AMPI, Jerusalem, Israel). Basic tension was adjusted with a vernier control to obtain maximal stimulated tetanic contraction force (usually about 10 g). Stability of the elicited contraction was monitored for one hour. Thereafter the medium was replaced every hour with 10 ml Ringer's medium containing increasing concentration (250, 500, 750, 1000, 1500 and 2500 nM) of D-tubocurarine (Sigma-Aldrich, Zwijndrecht, The Netherlands). Amplitude of contractions after equilibration of each D-tubocurarine concentration was cursor-measured off-line in Clampfit 9.0 (Axon Instruments), at 1 s after start of the each nerve stimulation train. We also stimulated the nerve with 15 pulses at 3 Hz at the end of each D-tubocurarine incubation period and cursor-measured the peak twitch tensions. Finally, D-tubocurarine was washed out and recovery of the tetanic contraction force was measured. Usually it was 5-10% higher than the force measured in the control period before D-tubocurarine addition. Measured forces in the successive D-tubocurarine periods were corrected for this increase, assuming a linear drift during the whole experiment.

Ex vivo *neuromuscular junction electrophysiology*

Phrenic nerve-hemidiaphragms, soleus and FDB muscles were dissected. Intracellular recordings of miniature endplate potentials (MEPPs, the spontaneous depolarizing events due to uniquantal ACh release) and endplate potentials (EPPs, the depolarization resulting from nerve action potential-evoked ACh release) were made at NMJs at 28 °C using standard micro-electrode equipment, as described previously (Plomp et al., 1992). At least 30 MEPPs and EPPs were recorded at each NMJ, and typically 5-15 NMJs were sampled per experimental condition per mouse. In FDB muscle, only MEPPs were measured. Muscle action potentials, mediated by Na^+ channels, were blocked by 3 μM of the selective muscle Na^+ channel blocker μ-conotoxin-GIIIB (Scientific Marketing Associates, Barnet, Herts, UK). In order to record EPPs, the nerve was stimulated supramaximally at 0.3 Hz and 40 Hz with either a bipolar electrode (phrenic nerve of diaphragm) or a suction electrode (tibial nerve of soleus). The amplitudes of EPPs and MEPPs were normalized to –75 mV, assuming 0 mV as the reversal potential for ACh-induced current (Magleby and Stevens, 1972). The normalized EPP amplitudes were corrected for non-linear summation according to (McLachlan and Martin, 1981) with an f value of 0.8. The quantal content at each NMJ, i.e. the number of ACh quanta released per nerve impulse, was calculated by dividing the normalized and corrected mean EPP amplitude by the normalized mean MEPP amplitude.

MEPPs were also recorded after addition of hypertonic medium (0.5 M sucrose Ringer's medium), in order to estimate the pool of ACh vesicles ready for immediate release (Stevens and Tsujimoto, 1995; Varoqueaux et al., 2005).

In order to assess the $Ca_V2.1$ channel dependence of ACh release, EPPs and MEPPs were also measured in the presence of 200 nM of the specific $Ca_V2.1$ blocker ω-agatoxin-IVA (Scientific Marketing Associates). Measurements were made following a 15 min pre-incubation with the toxin.

Morphological analyses

α-BUNGAROTOXIN STAINING AND IMAGE ANALYSIS - NMJ size at FDB muscles was determined by staining ACh receptors with fluorescently labelled α-bungarotoxin and quantification of the stained area, as described before (Kaja et al., 2005). Ten NMJs were quantified per muscle.

MUSCLE FIBRE COUNTING AND DIAMETER ANALYSIS - Soleus muscles were pinned out on loose blocks of silicone rubber, snap frozen in liquid nitrogen and subsequently embedded in TissueTek® (Bayer BV, Mijdrecht, The Netherlands). Transversal sections (12-18 μm) from the centre region of the muscle were cut on a Microm cryostat (Adamas Instruments BV, Leersum, The Netherlands) at –21° C and collected on poly-lysine coated slides. Sections were dried for 1 h at room temperature, fixed for 10 s in ice-cold acetone, stained for 10 s in 0.5% alkaline toluidine blue, dehydrated for 1 min each in a graded series of ethanol (50%, 70% 80%, 90%, 96%, 100%) and finally cleared in xylene. Sections were imbedded in Entellan mounting medium (Merck, Darmstadt, Germany) and viewed under a Zeiss Axioplan light microscope (Zeiss, Jena, Germany). Photos were taken with a digital microscope-camera and fibre diameter was measured using ImageJ software (U.S. National Institutes of Health, Bethesda, Maryland, USA). Stereological considerations were taken into account by defining the actual diameter of a single muscle fibre by the shortest distance measured. Twenty NMJs were quantified per muscle. The total number of fibres per section was counted from high resolution photographs of two different whole sections from each muscle. The muscle mean was used to calculate the grand mean ± S.E.M.

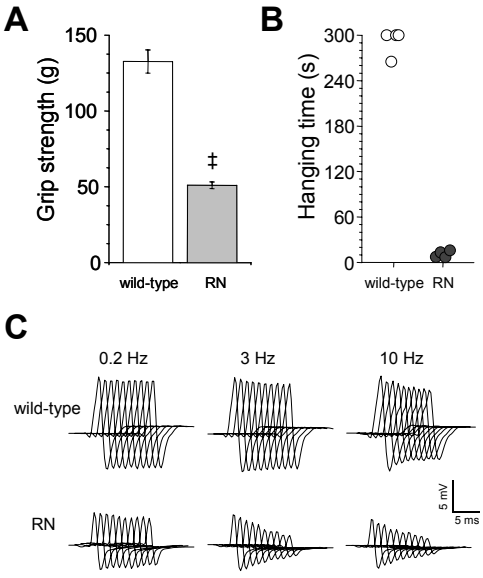

Figure 1. Reduced muscle strength and impaired electromyography of *rolling Nagoya* (RN) mice.
(**A**) Grip strength measurement of RN mice showed ~60% reduced muscle strength, compared to wild-type (n=4, p<0.001). (**B**) The inverted grid hanging test demonstrated fatigability in RN mice. Three of the four tested wild-type mice scored maximum recorded hanging times of 300 s. RN mice only managed hanging for 7-16 s (n=4). (**C**) Repetitive nerve stimulation electromyography (RNS-EMG) was performed on hind foot muscles of anaesthetized wild-type and RN mice (n=5). Representative traces of ten consecutive compound muscle action potentials (CMAP) amplitudes elicited at 0.2, 3 and 10 Hz are shown. Traces are spaced by 1 ms for easier visualization. RN mice had a smaller initial CMAP amplitude and increased decrement across all stimulation frequencies (0.2, 1, 3, 5, 10 Hz). Also see Table 1. ‡ p<0.001

Statistical analyses

Data is presented as mean ± S.E.M. Possible statistical differences were analysed with paired or unpaired Student's *t*-tests or ANOVA with Tukey's post-hoc test, where appropriate. N represents the number of mice measured. $P<0.05$ was considered to be statistically significant.

Results

Impaired in vivo *neuromuscular transmission causes muscle weakness and fatigue in RN mice*

Cacna1a mutations that cause severely reduced evoked transmitter release are likely to compromise successful transmission at the NMJ *in vivo*, as shown for some patients with EA2 mutations (Jen et al., 2001; Maselli et al., 2003a). In order to assess possible muscle weakness in RN mice, we measured grip strength and observed that the mean pulling force was reduced to 38% of wild-type force (Figure 1A). Whereas wild-type animals pulled 133 ± 8 g, RN mice only managed 51 ± 2 g (n=4, $p<0.001$).

Fatigability of limb muscles of RN mice was demonstrated in the inverted grid hanging test. While wild-type mice completed the maximum recording period of 300 s (except for one of the four tested mice, that scored 265 s), the RN mice (n=4) scored hanging times ranging from only 7-16 s (Figure 1B). Further analysis of weakness and fatigability with RNS-EMG revealed two abnormalities in RN mice. Firstly, the CMAP amplitude of the first stimulus in the trains was reduced by ~50%, compared to wild-type mice. This held for all five stimulation frequencies tested (n=5, $p<0.05$, Table 1, Figure 1C). Secondly, the CMAP decreased in amplitude during the trains. The maximal decrement was higher than at wild-type at every stimulation frequency. CMAP decrement increased with stimulation frequency, reaching 74 ± 7 % at 10 Hz (Table 1, Figure 1C). The decrement of RN CMAP area was found similarly increased ($p<0.05$, Table 1).

Table 1. Repetitive nerve stimulation electromyography (RNS-EMG) of *rolling Nagoya* (RN) mice.

CMAP parameter	Stimulation rate (Hz)	wild-type	RN	p
Initial amplitude (mV)	0.2	9.0 ± 1.8	5.1 ± 1.2	< 0.05
	1	8.8 ± 1.8	4.2 ± 0.9	< 0.05
	3	8.6 ± 1.9	4.4 ± 1.0	< 0.05
	5	8.3 ± 1.7	4.3 ± 1.3	< 0.05
	10	8.1 ± 1.7	4.1 ± 1.2	< 0.05
Maximal amplitude decrement (%)	0.2	1.3 ± 0.9	11.3 ± 2.9	< 0.05
	1	3.2 ± 1.8	29.6 ± 8.8	< 0.05
	3	4.2 ± 0.9	50.8 ± 17.8	< 0.05
	5	4.5 ± 2.4	52.7 ± 15.4	< 0.05
	10	7.1 ± 3.2	74.2 ± 6.6	< 0.001
Maximal area decrement (%)	0.2	0.6 ± 0.8	7.7 ± 3.5	0.095
	1	-0.3 ± 0.7	19.5 ± 7.1	< 0.05
	3	-0.2 ± 2.4	42.6 ± 16.9	< 0.05
	5	-2.0 ± 3.4	44.1 ± 18.3	< 0.05
	10	1.4 ± 2.6	66.2 ± 6.3	< 0.001

Compound muscle action potentials (CMAPs) recorded from hind feet of anaesthetized wild-type and RN mice upon supramaximal stimulation of the sciatic nerve. Initial CMAP amplitude was reduced by ~50% in RN mice (n=5, $p<0.05$) and showed a pronounced decrement upon repetitive stimulation, ranging from ~11% at 0.2 Hz to ~75 % at 10 Hz stimulation frequency.

Reduced safety factor of neuromuscular transmission at RN NMJs

With *ex vivo* diaphragm muscle contraction experiments we assessed the absolute contraction force of the RN diaphragm and the safety factor of neuromuscular transmission at its NMJs. At tetanic (40 Hz) nerve stimulation the absolute contraction force of RN muscles was somewhat (16%) smaller than that of wild-types, although this difference was not statistically significant (13.7 ± 0.9 and 16.3 ± 1.1 g, respectively, n=4, p=0.08). Tetanic contraction of RN muscles was more sensitive to D-tubocurarine than that of wild-type muscle (Figures 2A, B). For instance, the contraction force in the presence of 500 nM D-tubocurarine (normalized to the control force in absence of the drug) was 54.0 ± 5.2 and 85.6 ± 4.4% for RN and wild-type muscle, respectively, n=7, p<0.01, Figure 2A).

Also, the absolute twitch tension of RN muscles was somewhat (18%) smaller than that of wild-types, but again this difference was not statistically significant (3.1 ± 0.3 and 2.5 ± 0.2 g, respectively, n=7, p=0.14).

The rundown of 3 Hz evoked twitches (expressed as the ratio of the 15th and 1st twitch peak of a train) was more sensitive to D-tubocurarine at RN than wild-type muscles (Figure 2 D). For instance, in the presence of 750 nM D-tubocurarine it was 0.31 ± 0.06 and 0.84 ± 0.03 for RN and wild-type muscle, respectively, n=5, p<0.001.

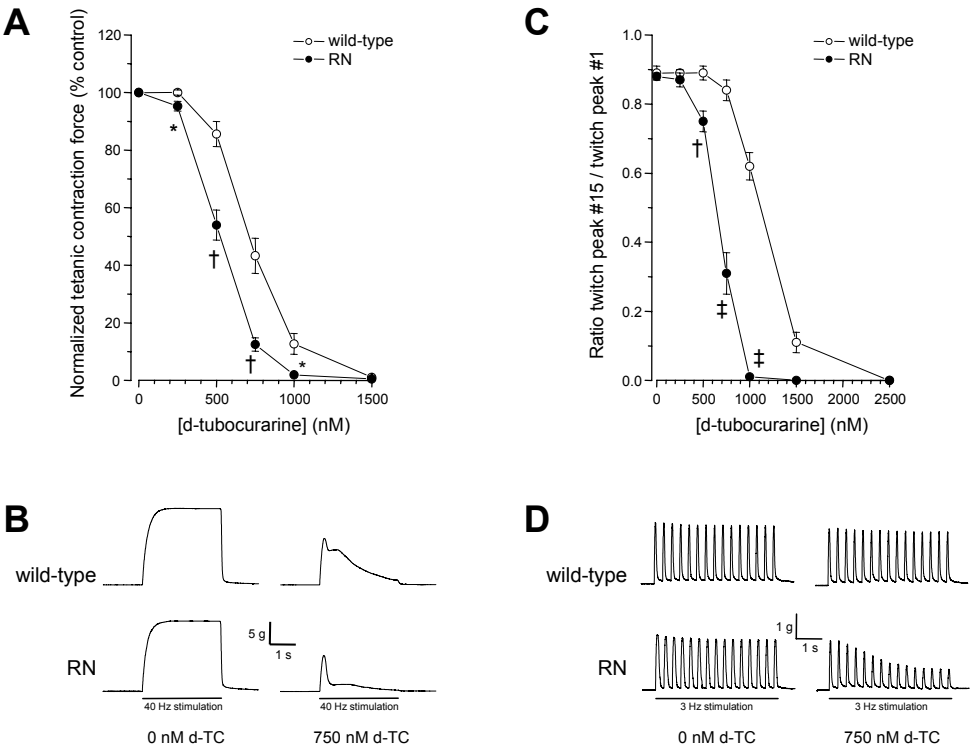

Figure 2. Reduced safety factor of neuromuscular transmission at *rolling Nagoya* (RN) NMJs.
(**A**) Increased sensitivity to D-tubocurarine (d-TC) of the tetanic *ex vivo* muscle contraction evoked by 40 Hz phrenic nerve stimulation of RN diaphragm muscle preparations, compared to wild-type (n=7). (**B**) Typical RN and wild-type contraction profiles upon 3 s supramaximal nerve stimulation before and in the presence of 750 nM D-tubocurarine. (**C**) Increased sensitivity to D-tubocurarine of the twitch contraction of RN muscles evoked by 15 phrenic nerve stimulations at 3 Hz (n=5). (**D**) Typical RN and wild-type twitch contraction profiles upon 5 s supramaximal nerve stimulation at 3 Hz before and in the presence of 750 nM D-tubocurarine.
* p<0.05, † p<0.01, ‡ p<0.001

The results of the *ex vivo* contractions experiments clearly demonstrate a reduced safety factor of neuromuscular transmission at RN diaphragm NMJs.

Ex vivo *electrophysiological analysis shows transmitter release defects at RN NMJs*

In order to determine in detail whether reduced ACh release at the NMJ was underlying the observed *in vivo* and *ex vivo* muscle weakness of RN mice, we performed micro-electrode measurements of EPPs and MEPPs at NMJs of diaphragm, soleus and FDB muscle.

Large increase of spontaneous ACh release - In diaphragm, mean MEPP frequency was increased compared to wild-type by ~200% at homozygous RN NMJs ($p<0.001$) and ~65% (although non-statistically significant, $p=0.08$) at heterozygous RN NMJs (1.26 ± 0.11, 2.05 ± 0.26 and 3.70 ± 0.39 s^{-1}, at wild-type, heterozygous and homozygous RN NMJs, respectively; n=5-8, 7-10 NMJs per muscle, Figure 3A). Thus, with respect to this parameter there is a strong tendency of RN gene-dosage dependency.

In order to estimate $Ca_V2.1$ channel contribution to spontaneous ACh release at RN NMJs, we tested the effects of 200 nM ω-agatoxin-IVA. The toxin reduced MEPP frequency by 45% ($p<0.05$), 60% ($p<0.05$) and 75% ($p<0.01$) to almost equal values: 0.65 ± 0.06, 0.79 ± 0.08 and 0.77 ± 0.14 s^{-1}, at wild-type, heterozygous and homozygous RN NMJs, respectively (n=3-5, 7-10 NMJs per muscle, $p=0.48$, Figure 3A).

The MEPP amplitude was ~1.0 mV under all conditions and did not differ between genotypes (n=5-8, 7-10 NMJs per muscle, $p=0.65$). Neither did MEPP rise times, decay times and half-width values (data not shown).

Severe reduction of evoked ACh release - When stimulating the phrenic nerve supramaximally at 0.3 Hz, the observed EPP amplitude was ~27 mV at wild-type, ~24 mV at heterozygous RN, and only ~16 mV at homozygous RN NMJs (Figures 3B, C). The quantal content, calculated from EPP and MEPP amplitudes, was reduced by ~20% ($p<0.05$) in heterozygous and ~50% ($p<0.001$) in homozygous RN NMJs, compared to wild-type (43.2 ± 2.2, 35.2 ± 2.2 and 23.0 ± 1.5 at wild-type, heterozygous and homozygous RN NMJs, respectively, n=5-8, 7-10 NMJs per muscle, Figure 3D). Kinetic parameters of EPPs, such as rise times, decay times and half-widths did not differ between genotypes (data not shown).

ω-Agatoxin-IVA (200 nM) reduced quantal content from 45.6 ± 2.9 to 2.4 ± 0.1 at wild-type NMJs (n=5, 7-10 NMJs per muscle, $p<0.001$, Figure 3D). At heterozygous RN NMJs, quantal contents were 35.2 ± 2.2 before and 2.9 ± 0.8 in presence of the toxin (n=5, 7-10 NMJs per muscle, $p<0.001$, Figure 3D), whereas at homozygous RN NMJs quantal contents decreased from 21.6 ± 1.2 to 1.0 ± 0.2 (n=3, 7-10 NMJs per muscle, $p<0.01$, Figure 3D). The reduction of quantal content was ~95% in all genotypes ($p=0.28$).

No change in hypertonic shock-induced ACh release - The hypertonic shock-induced ACh release at diaphragm RN NMJs did not differ from wild-type. MEPP frequency measured in 0.5 M sucrose Ringer's medium was 52.8 ± 9.4 and 59.0 ± 7.6 s-1 at RN and wild-type NMJs, respectively (n=5-6 muscles, 8-15 NMJs per muscle, $p=0.62$). This suggests an unchanged size of the readily releasable ACh vesicle pool.

Changed EPP amplitude rundown profile at high-rate stimulation at RN NMJs - Some effects of the RN mutation on transmitter release may only be unmasked at high intensity use of the channel. We, therefore, measured EPPs during 1s high-rate (40 Hz) nerve stimulation trains. Homozygous RN NMJs showed an EPP rundown profile that was different from that of wild-type and heterozygous NMJs (Figures 3E, F).

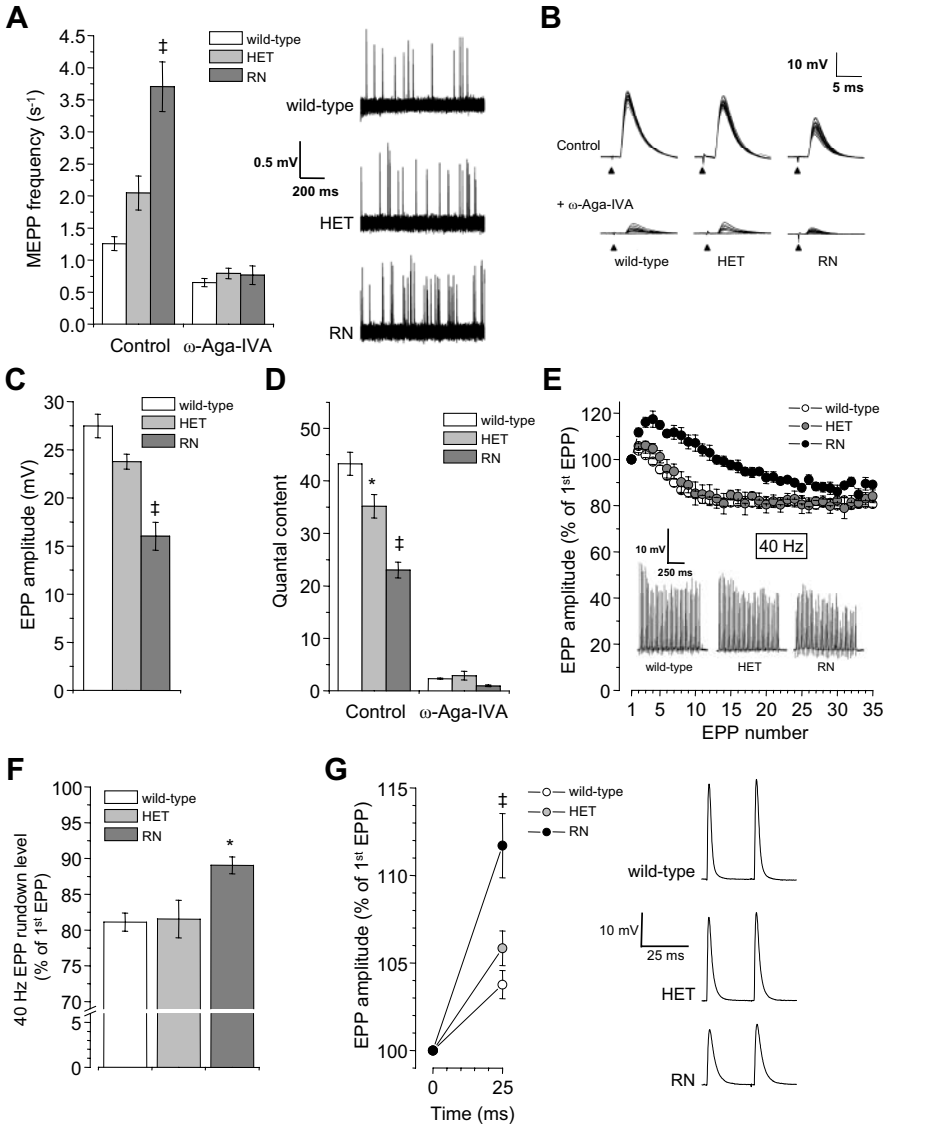

Figure 3. Impaired ACh release at hetero- (HET) and homozygous *rolling Nagoya* (RN) diaphragm NMJs.
(**A**) Increased spontaneous ACh release (MEPP frequency) at RN diaphragm NMJs, compared to wild-type, and the effect thereupon of 200 nM of the selective $Ca_V2.1$ channel blocker ω-agatoxin-IVA (n=3-8 muscles, 7-10 NMJs tested per muscle). ω-Agatoxin-IVA reduced MEPP frequency in all genotypes to almost equal values (~0.7 s^{-1}), showing that RN-mutated $Ca_V2.1$ channels were responsible for the increased MEPP frequency. At the right-hand side, traces of typical MEPP recordings are shown. For each genotype 10 superimposed sweeps of 1 s duration are plotted. (**B**) Typical examples of EPPs (20 superimposed traces) at low-rate 0.3 Hz stimulation, before (upper panel) and in the presence of ω-agatoxin-IVA (lower panel). Filled triangles indicate moment of nerve stimulation. (**C**) EPP amplitude (0.3 Hz stimulation) was ~40% smaller at homozygous RN NMJs (n=5-8 muscles, 7-10 NMJs per muscle, $p<0.001$). (**D**) Evoked ACh release (quantal content at 0.3 Hz stimulation) was reduced at heterozygous (by ~20%, $p<0.05$) and homozygous (by ~50%, $p<0.001$) RN NMJs (n=5-8 muscles, 7-10 NMJs per muscle). ω-Agatoxin-IVA reduced quantal content by ~95% in all three genotypes (n=3-5 muscles, 7-10 NMJs per muscle). (**E**) Homozygous RN NMJs show aberrant EPP amplitude rundown profile at high-rate (40 Hz) stimulation for 1 s. Averaged rundown profiles are shown, with EPP amplitude expressed as percentage of the first EPP in the train (n=5-8 muscles, 7-10 NMJs per muscle). Insets show typical examples of 40 Hz EPP train recordings. (**F**) Normalized EPP amplitude rundown level (mean EPP amplitude of the 21st-35th EPP, expressed as percentage of the first EPP) is higher (~90%) at RN than at wild-type (~80%) NMJs (n=5-8, 7-10 NMJs per muscle, $p<0.001$). (**G**) Increased 25 ms paired-pulse facilitation of EPPs at RN NMJs (n=5-8, 7-10 NMJs per muscle, $p<0.001$). Typical examples of paired-pulse evoked EPPs are shown at the right-hand side of the panel. $^{*}p<0.05$, $^{‡}p<0.001$, HET = heterozygous RN

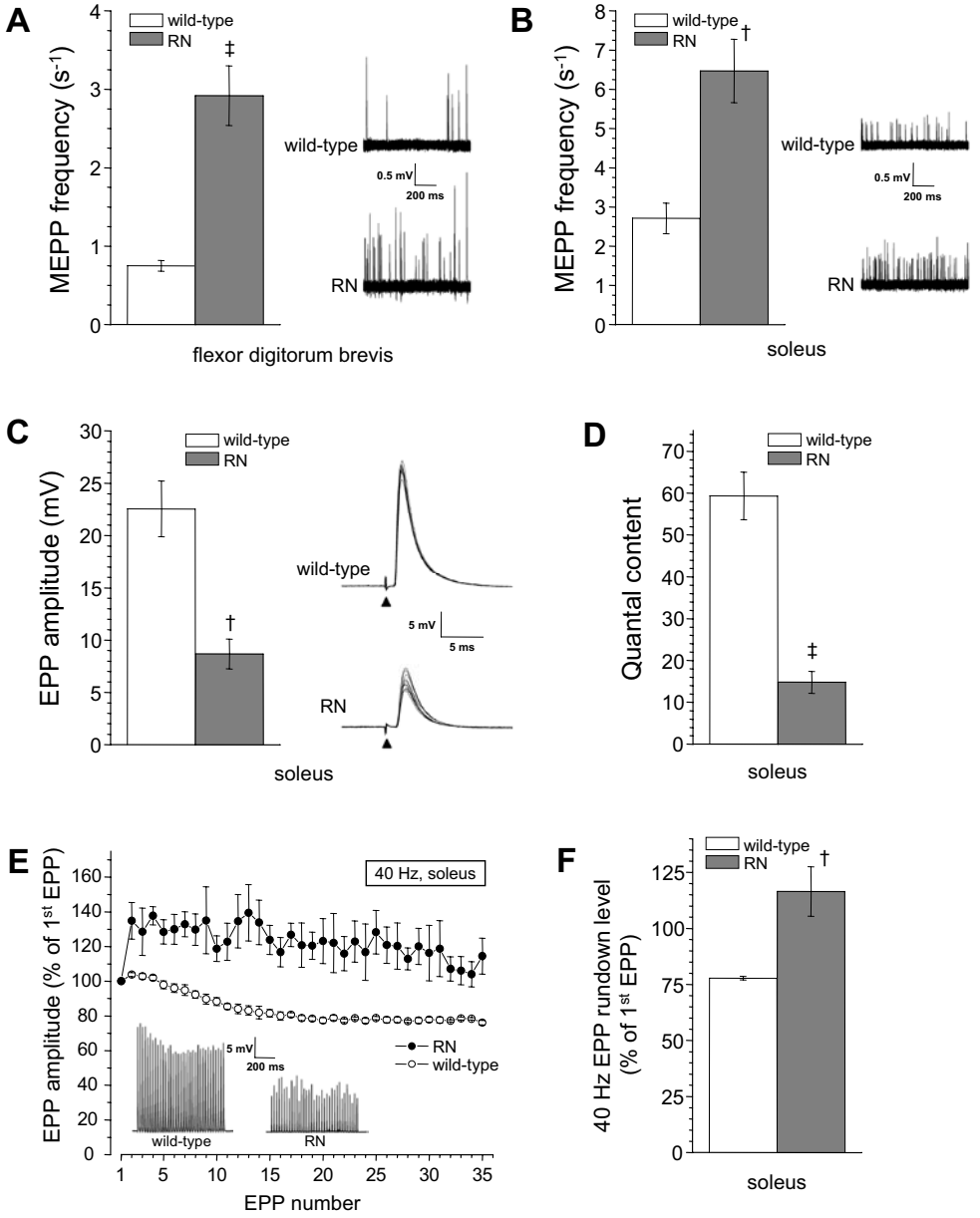

Figure 4. Impaired ACh release at *rolling Nagoya* (RN) flexor digitorum brevis (FDB) and soleus muscle NMJs.
(**A**) About 4-fold increased spontaneous ACh release at RN FDB NMJs (n=5 muscles, 10-15 NMJs per muscle, p<0.001). At the right-hand side, traces of typical MEPP recordings are shown. For each genotype 10 sweeps of 1 s duration are plotted superimposed. (**B**) About 2-fold increased spontaneous ACh release at RN soleus NMJs (n=4-5 muscles, 5-10 NMJs per muscle, p<0.01). At the right-hand side, traces of typical MEPP recordings are shown. For each genotype 10 superimposed sweeps of 1 s duration are plotted. (**C**) Reduced EPP amplitude at RN soleus NMJs (by 62%, n=4-5 muscles, 5-10 NMJs per muscle, p<0.01). Right-hand side of the panel shows typical EPPs recorded at 0.3 Hz stimulation. Ten superimposed sweeps are plotted. Filled triangles indicate moment of nerve stimulation. (**D**) The calculated quantal content was reduced by 75% at RN soleus NMJs (n=4-5 muscles, 5-10 NMJs per muscle, p<0.001). (**E**) Changed EPP amplitude profile at RN soleus NMJs at high-rate (40 Hz) stimulation for 1 s. Averaged profiles are shown, with EPP amplitude expressed as percentage of the first EPP in the train (n=4-5 muscles, 5-10 NMJs per muscle). Insets show typical examples of 40 Hz EPP train recordings. (**F**) Normalized EPP amplitude rundown level (mean EPP amplitude of the 21st-35th EPP, expressed as percentage of the first EPP) is higher (116%) at RN than at wild-type (78%) NMJs (n=4-5 muscles, 5-10 NMJs per muscle, p<0.001). † p<0.01, ‡ p<0.001

Subsequent to a rise to ~120% of the initial EPP amplitude of the train during the first five stimuli, EPP amplitude ran down to an average value of ~89 ± 1 % of the first EPP during the last 15 stimuli of the train (n=5-8, $p<0.05$ compared with wild-type, Figure 3F). The EPP rundown profile of heterozygous RN NMJs was not different from that of wild-type NMJs (average amplitude during the last 15 EPPs of the train was 82 ± 3 and 81 ± 1 % of the first EPP in the train, respectively, n=5-8, 7-10 NMJs per muscle, p=0.98, Figure 3F).

We looked in detail at the first two pulses of 40 Hz trains, which essentially is a test for 25 ms paired-pulse facilitation. This phenomenon of synaptic short-term plasticity was much larger at homozygous RN synapses (Figure 3G) than at either heterozygous RN or wild-type NMJs (11.7 ± 1.8, 5.8 ± 1.0 and 3.8 ± 0.8%, respectively, n=5-8, 7-10 NMJs per muscle, $p<0.001$).

Changes in ACh release at NMJs of RN soleus and FDB muscles

Slow- and fast-twitch muscle fibres have a different NMJ structure and function (Bewick, 2003). Thus, the effects of the RN mutation on transmitter release may differ amongst fibre types. Furthermore, NMJs in extremity muscles may differ from those in diaphragm (mixed population of slow- and fast-twitch fibres) due to different usage patterns. We therefore also determined ACh release at NMJs of soleus (slow-twitch) and the FDB (fast-twitch) muscle preparations of RN mice. We measured MEPP frequency in soleus and FDB NMJs and found increases, compared to wild-type, by 288% in FDB (n=5 muscles, 10-15 NMJs per muscle, $p<0.001$, Figure 4A) and by 139% in soleus NMJs (n=4-5 muscles, 5-10 NMJs per muscle, $p<0.01$, Figure 4B).

MEPP amplitudes in both muscle types of RN mice, compared to wild-type, showed a non-significant tendency for increase (by 20% in FDB, 1.36 ± 0.12 vs. 1.13 ± 0.11 mV, p=0.181, n=5 muscles and by 37% in soleus, 0.71 ± 0.07 vs. 0.52 ± 0.03 mV, p=0.06, n=4-5 muscles).

From soleus muscle NMJs we also recorded EPPs and calculated the quantal content. RN EPP amplitude, compared to wild-type, was reduced by 62% (n=4-5 muscles, 5-10 NMJs per muscle, $p<0.01$, Figure 4C) and quantal content by 75% (n=4-5 muscles, 5-10 NMJs per muscle, $p<0.001$, Fig 4D). The EPP amplitude profile at RN soleus NMJs during high-rate (40 Hz) nerve stimulation differed from wild-type in that EPPs increased to 120-140% of the first EPP at the first 20 stimuli and subsequently ran down to a level of 116 ± 11%, which was more than the plateau level of 78 ± 1% at wild-type NMJs (n=4-5 muscles, 5-10 NMJs per muscle, $p<0.01$, Figure 4F).

Thus, in general, effects of the RN mutation on ACh release at NMJs of soleus and FDB are comparable to those found at diaphragm NMJs.

Reduction of RN NMJ size and muscle fibre diameter

In view of their ~25% reduced body weight, RN mice might display some amount of muscle atrophy, which could (indirectly) influence NMJ function and RNS-EMG outcomes. We counted the number of muscle fibres in toluidine blue-stained cross sections of whole soleus muscle preparations. The total fibre number was 365 ± 33 and 351 ± 3 for wild-type and RN, respectively (n=3-4 muscles, p=0.74, Figure 5A). The diameter of RN soleus muscle fibres was 24% smaller than that of wild-type (20.8 ± 2.1 and 27.2 ± 1.5 μm, respectively, n=3-4 muscles, 20 fibres per muscle, $p<0.05$, Figure 5B).

We quantified NMJ size in FDB muscle using fluorescence microscopy. The α-bungarotoxin-stained area of RN NMJs was reduced by 24% compared to wild-type (189 ± 15 and 249 ± 14 μm^2, respectively, n=4 muscles, 10 NMJs per muscle, $p<0.05$, Figure 5 C, D).

Discussion

Neuromuscular function of RN mice and transmitter release properties at their NMJs were investigated here. Clinical electrophysiology demonstrated NMJ dysfunction as the most likely cause of the muscle weakness and fatigue found in grip strength and inverted grid hanging tests. Indeed, in *ex vivo* electrophysiological experiments we found that the R1262G amino acid change in presynaptic $Ca_V2.1$ Ca^{2+} channels severely affects neurotransmitter release at the NMJ: a 50-75% reduction of low-rate nerve stimulation-evoked release, accompanied by a ~3-fold increase of spontaneous ACh release. This is the first *Cacna1a* mouse mutant in which such opposing effects on spontaneous and evoked release are found. We assume that they result from a complex effect of the mutation on different functional channel parameters. The reduction of evoked ACh release at RN NMJs is apparently large enough to compromise the safety factor of neuromuscular transmission, and thereby, to cause (fatigable) muscle weakness. Below, our findings are discussed in the light of previous studies on RN-mutated $Ca_V2.1$ channel function and human diseases, in which lowered ACh release at NMJs leads to paralysis.

Reduction of evoked transmitter release

The low level of evoked ACh release at the RN NMJ may be caused by 1) reduced Ca^{2+} influx due to either reduced presynaptic $Ca_V2.1$ membrane insertion or reduced Ca^{2+} flux through the single channels, or 2) reduced efficacy of the translation of Ca^{2+} influx into transmitter release, or by combinations of these effects. The possibility of reduced Ca^{2+} influx is suggested from whole-cell recordings in a non-neuronal transfection system as well as in cultured cerebellar Purkinje cells from RN mouse brains (Mori et al*.,* 2000). In these studies, reduced current density and a reduced voltage sensitivity of activation were shown for RN. However, it is unclear whether these whole-cell findings can be directly translated to the behaviour of RN $Ca_V2.1$ channels in their specific presynaptic microenvironment.

In the only other study known to us on synaptic effects of the RN mutation (Matsushita et al*.,* 2002), strikingly opposing effects were found in different types of cerebellar synapses of RN mouse brain slices:

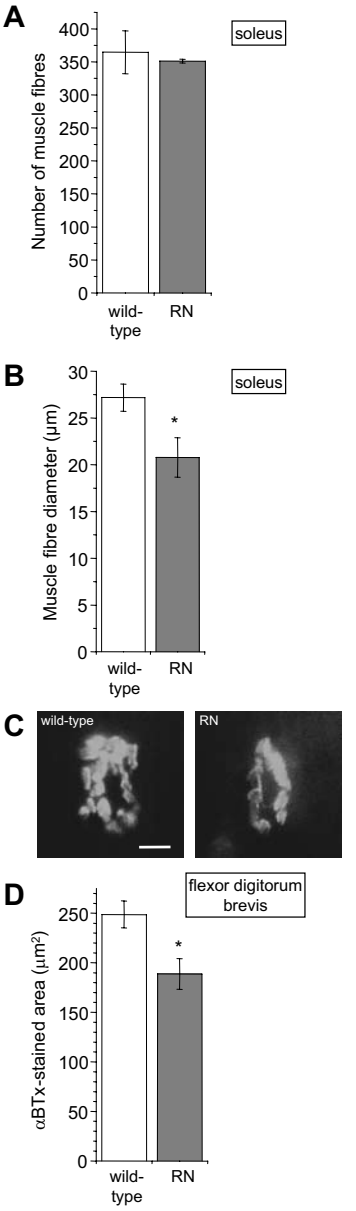

Figure 5. Morphological analyses.
(**A**) Total muscle fibre number, as determined from toluidene blue-stained cross-sections, is equal at RN and wild-type soleus muscle (n=3-4 muscles, p=0.74). (**B**) RN soleus muscle fibre diameter is 24% smaller than wild-type (n=3-4 muscles, 20 NMJs per muscle, $p<0.05$). (**C**) NMJs of RN FDB muscle, visualized by fluorescent α-bungarotoxin-staining, are somewhat smaller than in wild-type. Scale bar is 10 µm. (**D**) Quantification of fluorescent α-bungarotoxin-stained area. RN NMJs in FDB muscle are 24% smaller than wild-type (n=4 muscles, 10 NMJs per muscle, $p<0.05$). $^{*}p<0.05$

a large decrease of evoked synaptic postsynaptic currents in parallel fibre synapses and an increase in climbing fibre synapses. Apparently, RN mutation-induced changes in behaviour of $Ca_V2.1$ channels and the resulting impact on transmitter release depend considerably on the basic characteristics of the expressing synapse (e.g. release probability, Ca^{2+} dependency of release and overall synaptic strength), which differ extensively between parallel and climbing fibre synapses (Matsushita et al., 2002). The changes at the RN NMJ are rather similar to those at the parallel fibre cerebellar synapse: a large reduction in evoked transmitter release, with a concomitant increase of paired-pulse facilitation. It is yet unclear whether reduced expression of channels, reduced single channel Ca^{2+} flux, or a combination of both effects, contributes to reduced Ca^{2+} influx at RN presynapses. To our knowledge, single channel studies on RN-mutated $Ca_V2.1$ channels have never been performed.

The reduction of evoked release at RN NMJs contrasts the unchanged release (or even increased release, in low extracellular Ca^{2+}) at NMJs of *tottering*-, S218L- and R192Q-mutant mice, observed by us previously (Plomp et al., 2000; Van Den Maagdenberg et al., 2004; Kaja et al., Soc. Neurosci. Abstr., 2004; Kaja et al., 2005). This is in accordance with the oppositely directed shifts of activation voltages of RN channels (positive direction; Mori et al., 2000), *tottering* channels (no change; Wakamori et al., 1998) and S218L and R192Q channels (negative direction; Van Den Maagdenberg et al., 2004; Tottene et al., 2005). Therefore, change of activation voltage of these mutant channels is likely an important determinant of the final effect on evoked transmitter release, rather than some effect on membrane density of channels.

Reduced transmitter release can result from reduced release probability (p) of synaptic vesicles, or a reduced pool (n) of readily releasable vesicles (Stevens and Tsujimoto, 1995). Since we observed no change in pool size, as experimentally estimated from hypertonic sucrose-induced ACh release, the reduced evoked ACh release at RN NMJs most likely results from a reduced release probability (due to reduced Ca^{2+} influx). This may also explain the observed increase in paired-pulse facilitation (Zucker and Regehr, 2002).

In correlation with the reduced body weight of RN mice we observed ~25% reduced muscle fibre diameter and NMJ size. This suggests that a part of the reduction of evoked ACh release may be due to smaller RN NMJs, since size positively correlates with release (Harris and Ribchester, 1979). The tendency for somewhat increased MEPP amplitude at RN FDB and soleus NMJs may be explained by a higher electrical input resistance of smaller diametered muscle fibres (Katz and Thesleff, 1957).

The NMJ is well capable of expressing compensatory non-$Ca_V2.1$ type channels, as shown in $Ca_V2.1$ null-mutant (Urbano et al., 2003; Chapter 7) and *leaner* and *tottering* mice (Chapter 7; Kaja et al., 2006). At the RN NMJ, however, such compensation seems not present, since the selective $Ca_V2.1$ channel blocker ω-agatoxin-IVA reduced evoked ACh release equally across all genotypes by ~95%. This leads to the conclusion that chronic reduction of evoked ACh release by itself is not a trigger for compensatory expression of non-$Ca_V2.1$ channels.

Increased spontaneous ACh release

Spontaneous quantal ACh release, measured as MEPP frequency, was increased ~3-fold at RN NMJs, and was sensitive to ω-agatoxin-IVA as shown in both wild-type (45% reduction) and RN (75% reduction) diaphragm NMJs. This indicates that the increase was mainly caused by RN-mutated $Ca_V2.1$ channels, and that spontaneous ACh release at NMJs is partly controlled by ω-agatoxin-IVA-sensitive channels, suggesting the existence of low-voltage activated *Cacna1a*-encoded Ca^{2+} channels, as proposed by us before (Plomp et al., 2000).

Earlier we found increased spontaneous ACh release at NMJs of *tottering*- and R192Q-mutant NMJs (Plomp et al., 2000; Kaja et al., 2005), and recently also in S218L-mutated NMJs (Kaja et al., 2004; Chapter 4). As hypothesized before (Kaja et al*.,* 2005), this shared synaptic phenotype hints to a common mechanism and one possibility is a shift of activation potential of the mutated $Ca_V2.1$ channels in the negative direction. However, as mentioned above, the activation voltage of RN channels as determined in whole cell voltage-clamp experiments, is shifted in the *positive* direction (Mori et al*.,* 2000). One explanation may be that the RN mutation has opposing effects on the activation potential of putative low-voltage activated $Ca_V2.1$ channels (governing spontaneous ACh release) and on that of high-voltage activated ones (mediating evoked release). Possibly, the existence of alternative splicing $Ca_V2.1$ isoforms with specific biophysical properties that are affected differentially by the same mutation may be of importance here (Toru et al., 2000; Chaudhuri et al., 2004). Alternatively, RN-mutated channels may have an increased single channel conductance that causes some increase in Ca^{2+} influx at resting membrane potential but that the Ca^{2+} influx-reducing effect of a positive shift of activation voltage becomes the dominating effect upon activation by a presynaptic action potential.

RN is the first single amino acid change mutation of $Ca_V2.1$, in which opposite effects on spontaneous and evoked quantal transmitter release at the NMJ are found. Reduced evoked release with concomitantly increased spontaneous release was also found at NMJs of a muscle biopsy of one EA2 patient with a $Ca_V2.1$ truncation mutation. However, that condition is fundamentally different from RN, as reduced $Ca_V2.1$ channel-mediated release was partially compensated for by $Ca_V2.2$ channel contribution (Maselli et al., 2003a).

Impaired NMJ function leads to muscle weakness and fatigue in RN mice

The *ex vivo* tetanic contraction measurements at RN diaphragm muscles showed increased d-tubocurarine sensitivity. This demonstrates that the reduced evoked ACh release at the NMJ, as demonstrated in the electrophysiological experiments, causes a reduced safety factor of neuromuscular transmission.

With grip strength and inverted grid hang measurement we demonstrated *in vivo* muscle weakness and fatigue in RN mice, most likely caused by impaired NMJ function, as indicated from RNS-EMG measurements and confirmed by the *ex vivo* electrophysiological and muscle contraction experiments. The grip strength measurements may have been confounded by the ataxia of RN mice. However, ataxia is most prominent at the hind limbs and with their forepaws RN mice are well able to grab and hold the pulling bar of the measuring device. In comparison, *tottering* mice are also ataxic, but show no muscle weakness in the grip strength test (S. Kaja, unpublished observation), in line with *ex vivo* electrophysiological findings (Plomp et al., 2000) and therefore serve as negative control. Impaired *in vivo* NMJ function was indicated by reduced initial CMAP amplitude in the RNS-EMG studies of RN hind foot muscles, with pronounced decrements upon repetitive stimulation showing fatigability (also see below). However, it must be realized that a part of the ~50% reduction of initial CMAP amplitude in RN mice could possibly result from somewhat reduced muscle fibre diameter of hind foot muscles, similar to that shown in RN soleus. Taken together, these functional studies strongly suggest that the distinct gait abnormality of RN mice is caused by a combination of both ataxia and NMJ dysfunction-induced muscle weakness.

Shared features with LEMS and other presynaptic myasthenias

With respect to the *ex*- and *in vivo* NMJ electrophysiology, RN mice resemble human LEMS, a paralytic disorder characterized by anti-$Ca_V2.1$ auto-antibodies (Lennon et al*.,* 1995), which

is sometimes accompanied by cerebellar ataxia (Mason et al., 1997). *Ex vivo* electrophysiological analysis of synaptic signals at NMJ in muscle biopsies of LEMS patients has shown a reduced quantal content (Lambert and Elmqvist, 1971; J.J. Plomp, unpublished observations), similar to our observation at RN NMJs. In addition, high-rate evoked EPPs at LEMS NMJs also become strongly facilitated at the beginning of a stimulus train and show much less rundown in the later phase. Similar presynaptic defects were shown at NMJs of muscle biopsies of three congenital myasthenic syndrome patients without anti-$Ca_V2.1$ antibodies or identified *CACNA1A* mutation, but with symptoms of ataxia (Maselli et al*.,* 2001) and at biopsy NMJs of two EA2 patients with *CACNA1A* truncation mutations (Maselli et al., 2003a).

Results of the RNS-EMG tests of RN mice resembled typical findings in LEMS patients (AAEM Quality Assurance Committee, 2001; Sanders, 2003; Oh et al., 2005), as well as some EMG aspects of the presynaptic congenital myasthenic syndrome patients studied by Maselli and colleagues (2001). In LEMS, RNS-EMG is characterized by a low initial CMAP amplitude, a further decrease (the decrement) during low frequency nerve stimulation (1-10 Hz), and a pronounced increase to normal values during high frequencies (>10 Hz), proving that the initially low CMAP amplitude is due to some degree of blocked NMJs. RN mice showed low initial CMAP amplitudes and a decrement at low rates of stimulation. Unfortunately, movement artefacts precluded a meaningful CMAP analysis at higher stimulation frequencies. In man, such recordings require immobilization, but it proved unfeasible to immobilize the toes of the mice. We, therefore, cannot prove that the low initial CMAP amplitude is due to a synaptic block. Theoretically, the somewhat thinner muscle fibres may partly be responsible. However, the clear EPP amplitude facilitation during 40 Hz stimulation in the *ex vivo* electrophysiological analysis of soleus NMJs is compatible with CMAP increment.

While we have not performed stimulated single fibre electromyography in the RN mice, it is to be expected that such analysis will reveal increased jitter and the occurrence of 'blockings', as shown in LEMS (Chaudhry et al., 1991) and *CACNA1A*-mutated EA2 patients (Jen et al*.,* 2001; Maselli et al*.,* 2003).

Despite the different aetiology of the paralytic conditions in RN mice and LEMS patients, our studies suggest that RN mice can serve as a non-immunological model for LEMS, e.g. in order to perform *in vivo* and *ex vivo* NMJ drug studies. Possibly, the RN mouse also models aspects of EA2, in particular the NMJ impairments observed in patients with $Ca_V2.1$ truncation mutation. The general validity of this feature, however, remains to be established.

Gene dosage-dependency of effects

Heterozygous RN NMJs display an intermediate spontaneous ACh release, in-between wild-type and homozygous RN levels, and evoked release is somewhat lower than at wild-type NMJs. This indicates a gene dosage effect, which we also found for spontaneous ACh release at NMJs of *tottering* and R192Q knockin mice (Plomp et al., 2000; Kaja et al., 2005). The changes in gene dosage-dependent transmitter release parameters at CNS synapses are apparently not of sufficient magnitude to cause ataxia, as heterozygous RN mice have no overt symptoms, and muscle weakness is most likely prevented by the existence of a large safety factor of neuromuscular transmission (Wood and Slater, 2001). However certain, yet unknown, (experimental) conditions may exist that trigger ataxia in heterozygous RN mice.

Possible relevance to CNS synaptic function

Cerebellar synapses predominantly employ $Ca_V2.1$ channels for transmitter release (Forti et al., 2000; Stephens et al., 2001; Matsushita et al., 2002; Meacham et al., 2003). Changes in

release as observed at the RN NMJ may therefore be present at cerebellar synapses, disarranging neuronal network function and in this way contribute to ataxia. As mentioned above, reduced evoked transmitter release has been shown at cerebellar parallel fibre synapses (Matsushita et al., 2002). Besides, chronically increased spontaneous transmitter release at cerebellar synapses may lead to excessive pre- and postsynaptic Ca^{2+} influx, disturbing signalling pathways or initiating apoptosis or necrosis. Altered cerebellar synaptic morphology has been shown (Rhyu et al., 1999a), but conflicting reports exist as to whether RN cerebella show apoptosis and atrophy (Mori et al., 2000; Sawada et al., 2001; Suh et al., 2002). In addition to causing synaptic defects, RN-mutated $Ca_V2.1$ channels at cerebellar somata hamper action potential generation, presumably in an indirect fashion through reduced stimulation of Ca^{2+}-activated K^+ channels (Mori et al., 2000).

Possible relevance to CNS synaptic function

Cerebellar synapses predominantly employ $Ca_V2.1$ channels for transmitter release (Forti et al., 2000; Stephens et al., 2001; Matsushita et al., 2002; Meacham et al., 2003). Changes in release as observed at the RN NMJ may therefore be present at cerebellar synapses, disarranging neuronal network function and in this way contribute to ataxia. As mentioned above, reduced evoked transmitter release has been shown at cerebellar parallel fibre synapses (Matsushita et al., 2002). Besides, chronically increased spontaneous transmitter release at cerebellar synapses may lead to excessive pre- and postsynaptic Ca^{2+} influx, disturbing signalling pathways or initiating apoptosis or necrosis. Altered cerebellar synaptic morphology has been shown (Rhyu et al., 1999a), but conflicting reports exist as to whether RN cerebella show apoptosis and atrophy (Rhyu et al., 1999a; Mori et al., 2000; Sawada et al., 2001). In addition to causing synaptic defects, RN-mutated $Ca_V2.1$ channels at cerebellar somata hamper action potential generation, presumably in an indirect fashion through reduced stimulation of Ca^{2+}-activated K^+ channels (Mori et al., 2000).